Recent Developments in the Water Vapor Continuum

E. J. Mlawer, S. A. Clough, and P. D. Brown
Atmospheric and Environmental Research, Inc.
Cambridge, Massachusetts

D. C. Tobin
University of Wisconsin
Madison, Wisconsin

Introduction

A key development in the understanding of radiative transfer in the longwave was the introduction of the CKD continuum model (Clough et al. 1989), the success of which effectively ended speculation that there is significant longwave continuum absorption due to water vapor dimers or multimers. With the water vapor continuum defined as any observed absorption due to water vapor not attributable to the Lorentz line contribution[(a)] within 25 cm^{-1} of each line, a water vapor monomer line shape formalism was semi-empirically derived and consistently applied to all water vapor lines from the microwave to the shortwave. The success of this approach, which employed a common line shape for all spectral lines, led to the interpretation that water vapor continuum absorption was due to the intermediate and far wings of allowed transitions of the water vapor monomer. The current research effort modifies part of this interpretation, attributing a substantial portion of the continuum to collision-induced transitions of the water vapor monomer instead of the super-Lorentzian behavior of the intermediate wings of allowed transitions.

Observations and the CKD Continuum Model

The philosophy of a data-determined water vapor continuum has led to a series of revisions to the CKD continuum model as a result of high-resolution spectral observations, both from field campaigns and laboratory measurements. Most notable among these observations are those taken with the Atmospheric Emitted Radiance Interferometer (AERI) (Revercomb et al. 1996) at the Southern Great Plains (SGP) site of the Atmospheric Radiation Measurement (ARM) Program, which has allowed stringent validation of the CKD model in certain spectral regions, especially the 9.6-µm atmospheric window. Figure 1 illustrates the initial and most recent versions of the self-broadened water vapor continuum, which differ in most spectral regions. The differences between CKD_0 and CKD_2.4 are (from low frequency to high frequency): a) in the microwave, extrapolation from AERI validations in the ν_2 band led to a large increase; b) in the atmospheric window (700 cm^{-1} to 1200 cm^{-1}), adjustments were made as a result of AERI validations and the tropical measurements due to Han et al. (1997); and c) in the ν_2

(a) Minus the value of the Lorentz lineshape at 25 cm^{-1} from line center.

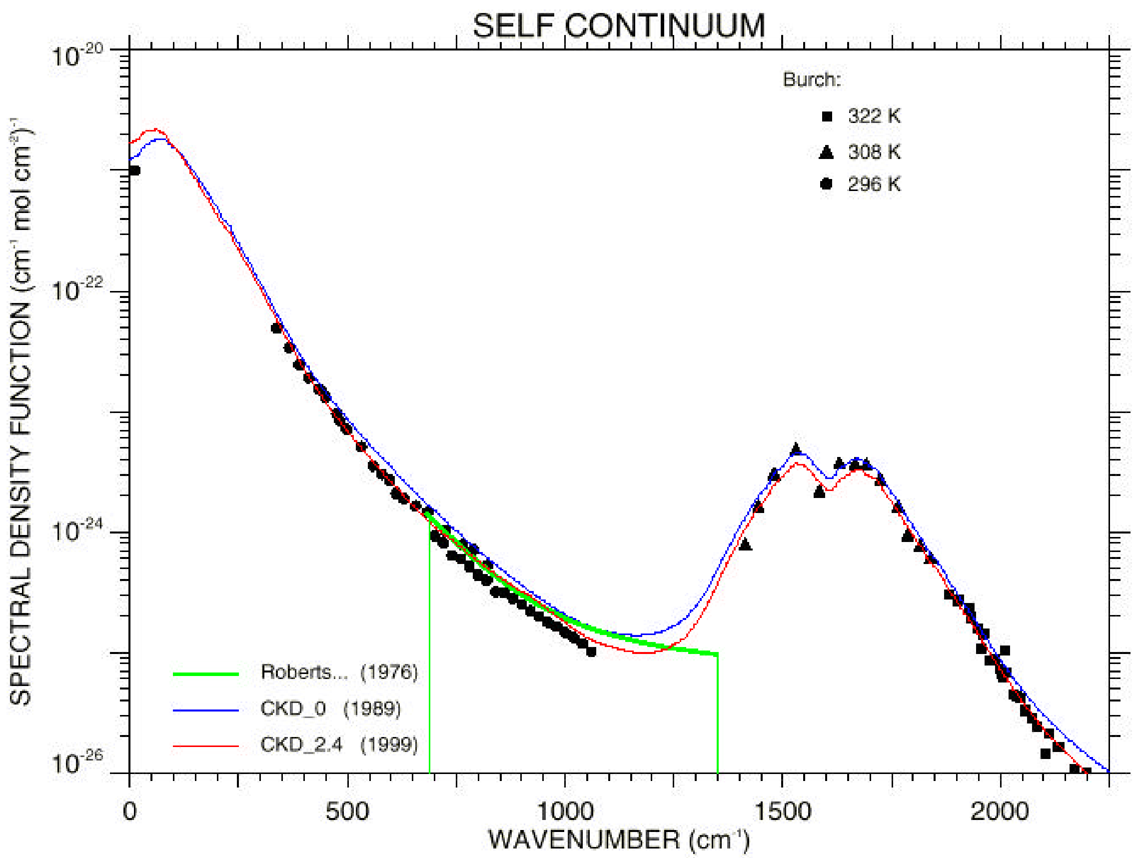

Figure 1. The CKD_0 (upper at 1500 cm^{-1}) and CKD_2.4 (lower at 1500 cm^{-1}) self-broadened water vapor continuum models for the longwave spectral region. Also shown for reference are the Roberts et al. (1976) continuum model and the laboratory measurements due to Burch (1981).

band (1300 cm^{-1} to 1800 cm^{-1}), AERI validations and greater confidence in the measurements of Burch (1981) led to a decrease in continuum values. Especially interesting is the feature centered at 930 cm^{-1} (Han et al. 1997), which, unlike the other features in the self-continuum model, cannot be attributed to water vapor monomer transitions. This bumplike feature, which scales quadratically with water vapor abundance and at its peak is responsible for ~30% of the self-continuum absorption, is possibly due to water vapor multimers.

Figure 2 shows the first and current versions of the CKD foreign-broadened continuum. The lowering of the foreign continuum on both sides of the ν_2 band were effected to provide better agreement with AERI measurements. The most recent revision to the model is in the spectral range 300 cm^{-1} to 600 cm^{-1} and is a result of measurements (Tobin et al. 1999) by an extended range AERI that were taken as part of the Surface Heat Budget of the Arctic (SHEBA) campaign (Moritz et al. 1993). The cold and dry conditions present on the day of this observation created an opening in this usually opaque spectral window, allowing the determination of foreign continuum coefficients. Figure 3 shows this observation, as well as the improved residuals obtained when using CKD_2.4 in comparison with CKD_2.2.2 and no

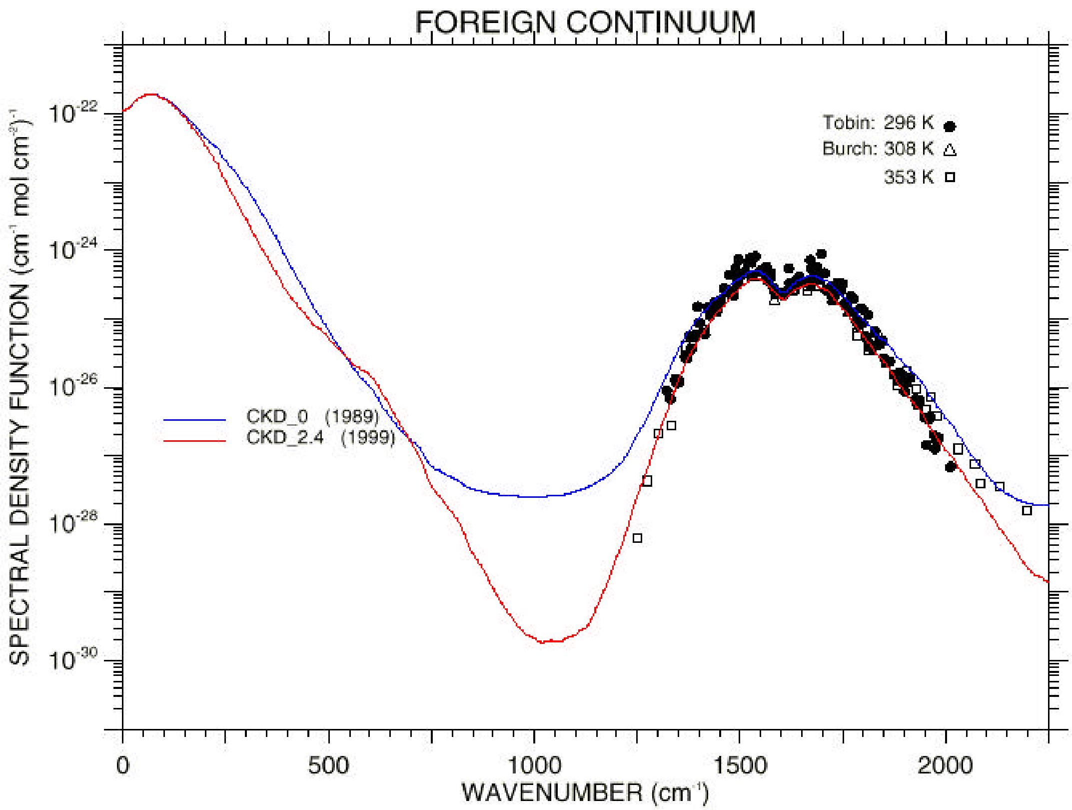

Figure 2. The CKD_0 (upper at 1500 cm^{-1}) and CKD_2.4 (lower at 1500 cm^{-1}) foreign-broadened water vapor continuum models for the longwave spectral region. Also shown for reference are the laboratory measurements due to Burch (1981) and Tobin et al. (1996).

continuum. The weaker foreign continuum in this spectral region in CKD_2.4 leads to an increase of ~1 W/m^2 in outgoing longwave radiation relative to previous versions of the foreign continuum (Mlawer et al. 1998), mostly due to decreased absorption by water vapor in the upper troposphere. This illustrates the value in using observations obtained in cold and dry conditions, such as those common at higher latitudes, as surrogates for observations in the upper troposphere.

Theoretical Considerations

It is important to note that every revision to the CKD continuum model contained adjusted values of the continuum coefficients in limited spectral ranges, but did not follow from a revision of the originally derived line shape formalism. In the CKD_0 formalism, all continuum absorption is attributed to allowed water vapor transitions. A large increase in the value of the Lorentz line shape in the intermediate line wing was employed to obtain agreement with laboratory data (Burch 1981), especially in the center of the ν_2 band. This super-Lorentzian intermediate-wing behavior had no physical justification, in contrast to the sub-Lorentzian behavior of the CKD_0 line shape in the far wing, which follows from the assumption of a finite duration of collision involving the radiating water vapor molecule.

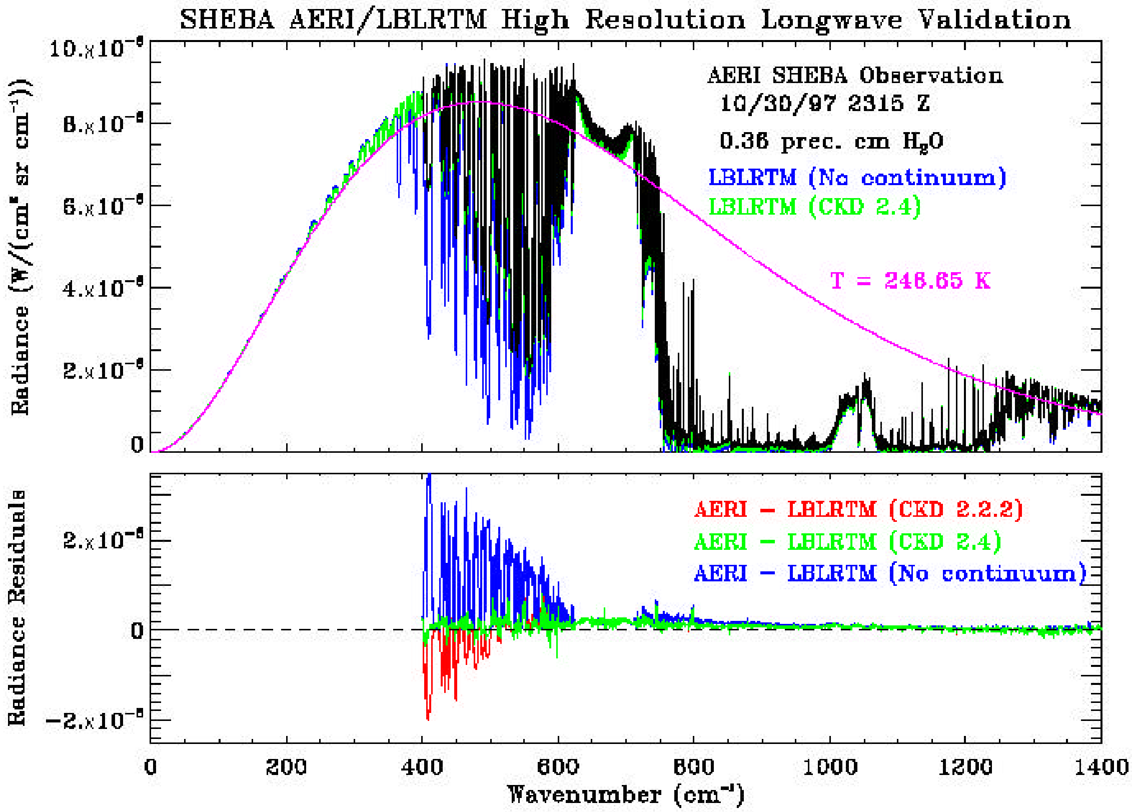

Figure 3. (upper panel) The downwelling radiance as a function of wavenumber (black curve) measured by the AERI as part of the SHEBA campaign, (blue curve) calculated using LBLRTM with no continuum, and (green curve) calculated with LBLRTM using CKD 2.4. (lower panel) The difference in downwelling radiance between the observation and LBLRTM calculations using (blue curve) no continuum, (green curve) CKD_2.4, and (red curve) CKD_2.2.2.

The increase in absorption associated with the super-Lorentzian intermediate wing of the CKD_0 line shape is troubling and does not pass scrutiny as the most straightforward approach to model the increased in-band absorption. Evidence for a more compelling explanation can be seen by subtracting the continuum contribution (as defined above) resulting from a line shape with a purely Lorentzian line center and intermediate wings and sub-Lorentzian far wings from measurement-determined continuum coefficients. The residual obtained is suggestive of an absorption band due to collision-induced transitions, which have halfwidths large enough (due to the briefness of the deformative collision) to provide the observed absorption at the center of the ν_2 band where the allowed transitions are very weak. A revised formalism for the water vapor continuum needs to account for these collision-induced effects.

Recent laboratory measurements (Tobin et al. 1996) have provided continuum coefficients at a number of spectral points in the ν_2 band. This study improved upon the previous measurements by Burch (1981) since it not only probed the continuum at frequencies previously measured by Burch (1981), but also provided continuum coefficients in microwindows too small to be examined with Burch's (1981) lower resolution instrument. These new measurements have proved valuable for their increased spectral coverage, but, equally importantly for their strong verification of the scaling properties of the continuum with respect to water vapor abundance: linear for the foreign continuum, and quadratic for the self continuum.

Analysis of the measurements presented in Tobin et al. (1996) indicated that the self- and foreign-broadened continua had a relatively high-frequency component, a feature before reported. However, it now appears that these features can be more simply explained by the use of inaccurate halfwidths when the local line contribution was removed from the data. A preliminary analysis suggests that increasing the high-resolution transmission (HITRAN) self-broadened halfwidths by 15% to 20% and the foreign-broadened halfwidths by ~5% would eliminate the higher frequency behavior of the derived continuum coefficients. These increases are currently within the uncertainty in the knowledge of these halfwidths. An effort is presently under way in the spectroscopic community to obtain a more accurate determination of these halfwidths (C. Camy-Peyret, personal communication).

The Tobin et al. (1996) measurements are currently being reanalyzed to determine the adjustment that has to be made to the halfwidth of each spectral line in order to remove the higher-frequency component. After that has been accomplished, a revised formulation will be developed that will include

- a component to account for allowed transitions, which will be characterized by a line shape with a sub-Lorentzian far wing

- a low-frequency component due to collision-induced transitions to provide agreement at the centers of the pure rotation and ν_2 bands.

It is important to note that, due to these multiple quantum mechanical sources of the continuum, these components must be added together in this formulation, in contrast to the multiplicative 'χ-factor' approach used previously. Still, the clearly causal relationship between the water vapor monomer line absorption spectrum and the collision-induced absorption spectrum (given by the second of the two components listed above) validates the main conclusion expressed by Clough et al. (1980; 1989) that the continuum (with the exception of the feature at 930 cm^{-1} that is included in the self-continuum) is due to the water vapor monomer.

References

Burch, D. E., 1981: Continuum absorption by H_2O, AFGL-TR-81-0300.

Clough, S. A., F. X. Kneizys, R. W. Davies, R. Gamache, and R. H. Tipping, 1980: Theoretical line shape for H_2O vapor, application to the continuum. In *Atmospheric Water Vapor,* A. Deepak, T. D. Wilkerson, and L. H. Ruhnke, eds. Academic Press, London, 25-46.

Clough, S. A., F. X. Kneizys, and R. W. Davies, 1989: Line shape and the water vapor continuum. *Atmos. Res.*, **23**, 229-241.

Han, Y., J. A. Shaw, J. H. Churnside, P. D. Brown, and S. A. Clough, 1997: Infrared spectral radiance measurements in the tropical Pacific atmosphere. *J. Geophys. Res.*, **102**, 4353-4356.

Mlawer, E. J., S. A. Clough, P. D. Brown, and D. C. Tobin, 1998: Collision-induced effects and the water vapor continuum. In *Proceedings of the Eighth Atmospheric Radiation Measurement (ARM) Science Team Meeting*, DOE/ER-0738, pp. 503-511. U.S. Department of Energy, Washington, D.C.

Moritz, R. E., J. A. Curry, A. S. Thorndike, and N. Untersteiner, editors, 1993: Prospectus, SHEBA, a research program on the surface heat budget of the Arctic Ocean. *ARCSS-OAII Report #3*, 34 pp., printed by ASRCSS-OAII Sci. Mgt. Ofc., Univ. of Washington, August 1993.

Revercomb, H. E., F. A. Best, R. O. Knuteson, B. A. Whitney, T. P. Dirkx, R. G. Dedecker, R. K. Garcia, P. van Delst, and W. L. Smith, 1996: Atmospheric Emitted Radiance Interferometer (AERI), Part I: Status, basic radiometric accuracy, and unexpected errors and solutions. Paper presented at the Sixth ARM Science Team Meeting, San Antonio, TX, March 4-7, 1996.

Roberts, R. E., J.E.A. Selby, and L. M. Biberman, 1976: Infrared continuum absorption by atmospheric water vapor in the 8-12 μ window. *Appl. Opt.*, **15**, 2085-2090.

Tobin, D. C., L. L. Strow, W. J. Lafferty, and W. B. Olson, 1996: Experimental investigation of the self- and N_2-broadened continuum within the ν_2 band of water vapor. *Appl. Opt.*, **35**, 4724-4734.

Tobin, D. C., F. A. Best, P. D. Brown, S. A. Clough, R. G. Dedecker, R. G. Ellingson, R. K. Garcia, H. B. Howell, R. O. Knuteson, E. J. Mlawer, H. E. Revercomb, J. F. Short, P. F. van Delst, and V. P. Walden, 1999: Downwelling spectral radiance observations at the SHEBA ice station: Water vapor continuum measurements from 17-26 μm. *J. Geophys. Res.*, **104**, 2081-2092.